Biosensors and Bioelectronics 24 (2009) 2804–2809

Contents lists available at ScienceDirect

Biosensors and Bioelectronics

journal homepage: www.elsevier.com/locate/bios

Novel U-bent fiber optic probe for localized surface plasmon resonance based biosensor

V.V.R. Sai[a], Tapanendu Kundu[b], Soumyo Mukherji[a,c,d,*]

[a] School of Biosciences and Bioengineering, IIT Bombay, Mumbai 400076, India
[b] Department of Physics, IIT Bombay, Mumbai 400076, India
[c] Centre for Research in Nanotechnology and Science, IIT Bombay, Mumbai 400076, India
[d] Centre of Excellence for Nanoelectronics, IIT Bombay, Mumbai 400076, India

ARTICLE INFO

Article history:
Received 18 November 2008
Received in revised form 18 January 2009
Accepted 9 February 2009
Available online 20 February 2009

Keywords:
Gold nanoparticles
Localized SPR biosensor
Absorbance sensor
U-bent fiber optic probe

ABSTRACT

The aim of this study is to develop an optical absorbance based biosensor suitable for wide scale use in resource-poor locales. A sensor for sensitive measurement of refractive index (RI) with the help of optical absorbance properties of gold nanoparticles (GNP) coupled to an efficient optical transducer in the form of a U-bent fiber optic probe is described. A U-bent probe was fabricated by a simple procedure. The absorbance due to the localized surface plasmon resonance (LSPR) of fiber-bound GNP was found to be linear to refractive index changes between 1.33 and 1.35. A U-bent probe of 200 μm diameter with a bend radius of 0.75 mm gave rise to a sensitivity of 35 ΔA/RIU at 540 nm. The resolution of the sensor probe was 3.8×10^{-5} RIU. Label-free biosensing was demonstrated using these probes with the help of IgG–anti IgG as bioreceptor–analyte pair.

1. Introduction

In recent times, chemical and biochemical sensors based on surface plasmon resonance (SPR) and other label-free techniques have been developed by many researchers and subsequently commercialized (Homola, 2006; Cooper, 2006). Applications in different fields ranging from medical diagnostics to environmental monitoring have been explored (Homola, 2008). During the last decade, extensive research in the field of nanotechnology has enabled development of new biosensing techniques using metal colloids.

Nanoparticles of noble metals such as gold and silver exhibit optical absorption and scattering properties in UV–visible region termed as localized surface plasmon resonance (LSPR) (Jain et al., 2007). The extinction band due to LSPR is influenced by the size, shape and composition of nanoparticles and most importantly by the surrounding environment. Refractive index changes taking place at the surface of the nanoparticles result in changes in absorbance and a red shift in absorbance peak (λ_{max}). These properties of Au and Ag nanoparticles have been utilized in liquid phase as well as monolayers coated on glass/quartz substrates to develop colorimetric biosensors (Englebienne, 1998; Grabar et al., 1995; Okamoto et al., 2000; Nath and Chilkoti, 2002; Lin et al., 2006; Frederix et al., 2003). However, these sensors have been limited by the RI sensitivity in order of several units of ΔA/RIU. Different methodologies of localized SPR with improved sensitivity have been reported. Tamiya and colleagues have developed gold-capped silica/polystyrene nanoparticles coated substrates for biosensing and observed better absorbance sensitivity (Endo et al., 2005).

Absorbance response of gold nanoparticles (GNP) based sensors can be further enhanced by coating GNPs on an efficient absorbance based sensor. Optical fiber probes have been exploited in an attempt to enhance the sensitivity of LSPR based biosensor by using fiber optic evanescent-wave sensing scheme (Chau et al., 2006). GNP coated straight fiber probes have been used for demonstrating chemical and biochemical sensing. In another configuration, gold colloids have been adsorbed on the grating portion of long period fiber grating (Tang et al., 2006). A miniaturized fiber optic biosensor with better refractive index sensitivity has been demonstrated by coating the distal end of a 50 μm fiber core diameter with gold nanoparticles (Mitsui et al., 2004). A fiber-optic biosensor based on the generation of localized surface plasmons (LSP) near a nano fiber tip has been proposed. The nano-optical fiber biosensor was made by shaping the fiber to form a taper with a tip size less than 100 nm. A sensitivity of ∼4800 (% RIU^{-1}) in the intensity measurement has been reported (Wei et al., 2006).

It is known that evanescent wave based absorbance sensitivity of bare (uncoated) fiber sensor probes can be increased by modifying the probe geometry. Different fiber optic probe designs including straight, U-bent, tapered tip, and biconical tapers have been employed in development of absorbance based bio/chemical sen-

* Corresponding author. Tel.: +91 22 25767767; fax: +91 22 25723480.
E-mail address: mukherji@iitb.ac.in (S. Mukherji).

0956-5663/$ – see front matter © 2009 Elsevier B.V. All rights reserved.
doi:10.1016/j.bios.2009.02.007

sors (Leung et al., 2007). We have chosen U-bent probes due to their sensitivity, compactness, ease in fabrication, and possibly higher compatibility with instrument configurations. U-bent probes have been demonstrated to have a 10-fold improvement in absorbance sensitivity over straight probes (Gupta et al., 1996). This may be due to the creation of higher order modes from lower order modes concentrated along the centre of optical axis of a bent fiber. It results in a significant increase in penetration depth of the evanescent field at the bent region and beyond in the direction of light propagation (Khijwania and Gupta, 1998), (Littlejohn et al., 1999). However, as per our knowledge, no study has been published on combining the advantages of GNP based detection with enhanced evanescent wave absorption exhibited in bent optical fiber probes.

In this report, we describe the development of novel LSPR biosensor using GNP coated U-bent fiber optic probes. A simple procedure was used to fabricate U-bend probes from uncladded straight fibers. A complete optical set-up involved a fiber sensor probe, a light emitting diode (LED) and a detector that operates in visible range along with signal conditioning and processing electronics. In the present studies, a spectrometer was used for analyzing the output obtained from the fiber probes. Promising results were obtained using GNP coated U-bent sensor probes. It may be envisaged that simple photodetectors can be used for reduction of cost and complexity in field studies.

2. Experimental

2.1. Reagents and materials

Tetra chloro aurate ($HAuCl_4$), Cystamine ($HS\text{-}C_2H_4\text{-}NH_2$), Phosphate buffer saline (PBS) were obtained from Sigma. Aminosilane (N-[3-trimethoxy silyl]propyl) ethylene diamine, >99%) was procured from Aldrich. Glutaraldehyde ($OHC\text{-}C_2H_4\text{-}CHO$) was obtained from Fluka. Trisodium citrate and acetic acid were purchased from SD fine chemicals, India. All antibodies, human IgG (HIgG), rabbit IgG (RIgG) and goat anti-human IgG-affinity purified (GaHIgG) and bovine serum albumin (BSA) were obtained from Bangalore Genei, India. All the reagents were of analytical grade. All solutions were prepared using de-ionized (DI) water obtained from a MilliQ filtration system. Optical fibers of diameter 200 μm and NA = 0.37, obtained from Thorlabs®.

2.2. Synthesis of gold nanoparticles

Gold nanoparticles used in these experiments were synthesized by following a procedure described by Turkevich et al. (1951). 50 mM $HAuCl_4{\cdot}3H_2O$ in DI water was prepared as a stock solution. 0.2 mL of 50 mM gold chloride solution was added to 39.15 mL of DI water and heated until it began to boil. 0.647 mL of 5 mg/mL sodium citrate trihydrate solution was added as soon as boiling commenced. Heating was continued until the solution turned pale purple in colour. Then the solution was removed from the hot plate and allowed to cool to room temperature. The molar ratio of citrate to gold was 1.1. The average size of the synthesized nanoparticles was 40 nm. The absorbance peak for gold nanoparticles solution was at 530 nm as shown in Fig. 1.

2.3. Fiber probe preparation

The fibers were cut into 40 cm long pieces. A 2 cm length in the middle of the fiber was decladded to expose its core. The buffer and cladding were stripped by using a sharp surgical blade. The terminal ends of optical fiber were polished by using emery papers with 5, 1 and 0.3 μm roughness in sequential order. We attempted bending of 200 μm diameter fibers using a simple wax candle flame, in contrast to propane or oxy-butane flames used by earlier investigators (Gupta et al., 1996) and succeeded in obtaining bend radii as small as 0.5 mm with satisfactory repeatability (Figure S-3). We used different portions of the flame for fabricating different bend radii, as opposed to controlling the ratio in gas mixtures required in the case of propane or oxy-butane flames. The bluish flame at the bottom of the flame was used to obtain radius of 0.5–0.75 mm. The region at the tip of the flame was used for radius of 1 mm and above. The bent portions were observed under an optical microscope and diameters were measured from the images of U-bent probes by using Axiovision® software (Carl-Zeiss®). The core diameter of the fiber was found to be uniform at the bent portion.

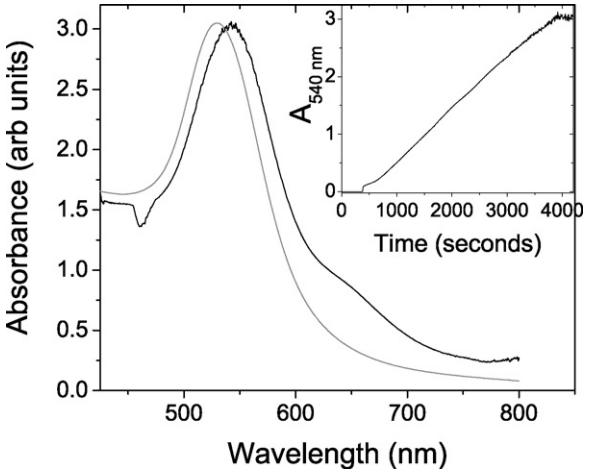

Fig. 1. Comparison of absorbance spectrum obtained from fiber probe due to GNP binding (black) with that of GNP solution (gray); Inset: real-time response observed at 540 nm due to binding of gold nanoparticles to the fiber probe of bend radius 0.75 mm.

2.4. Optical set-up

The optical set-up for absorbance measurements consists of a white light emitting diode (5W4HCA-H20-ULTRA, 19.0–25.0 cd at 20 mA, view angle 20°, 5 mm clear epoxy from Roithner LaserTechnik, Austria) with spectral emission between 430 and 700 nm and a fiber optic spectrometer (Scheme 1). One of the polished ends of prepared fiber sensor probe was held by a fiber chuck in fiber coupler (Newport®, USA). Light from LED was focused through a

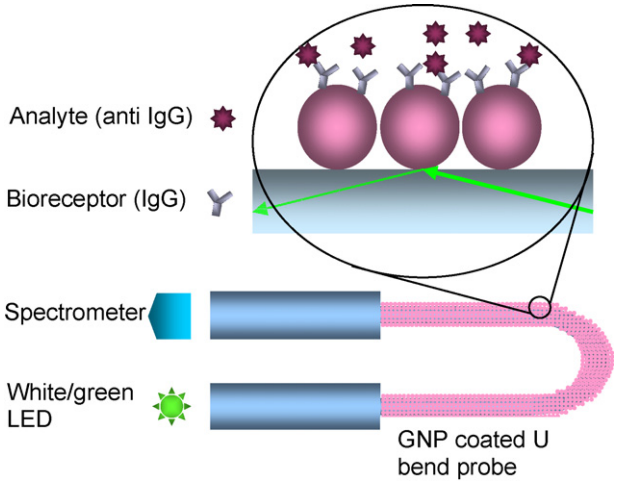

Scheme 1. Optical set-up and sensing scheme used for experiments with U-bent fiber optic probe.

microscopic objective lens, 40×, 0.6 NA, onto the fiber end. The decladded fiber sensor portion was held within a custom-made glass capillary channel with inlet and outlet ports. The other end of the probe was held by using a fiber positioner. Light from this end was collected into a fiber optic spectrometer (USB 4000, Ocean Optics®). A schematic giving the details of experimental set-up is shown in Figure S-4 of Supplementary Material. Binding events taking place on fiber probe surface were monitored as absorbance changes at 540 nm in real-time and the full absorbance spectra were recorded at the end of the experiments. Signal-to-noise (SNR) was improved by averaging 100 consecutive spectra. Spectrasuite® software was used to acquire absorbance spectra and real time absorbance changes at a particular wavelength.

2.5. Functionalization of fiber probes

Fiber probes were functionalized with amino silane to bind the gold nanoparticles to the sensor surfaces. Substrates were treated in sulphochromic solution (100 mL of conc. H_2SO_4 added to 500 μg of $K_2Cr_2O_7$ in 1 mL of DI water) for 8–10 min thoroughly and then washed twice in DI water. This creates (additional) silanol sites (Si-OH) on the surface for covalent binding of aminosilane molecules. Fiber probes were dehydrated at 115 °C for 2 h. They were then dipped in 1% Silane prepared in ethanol: acetic acid (10:4) solvent for 3–5 min in Argon ambient. Acetic acid helps in restricting the formation of multi-layers of silane that could lead to aggregation of gold nanoparticles on sensor surfaces (Prasad, 1999). Substrates were washed in absolute ethanol after silane treatment and condensed by heating at 110 °C for 20 min.

3. Results

3.1. Formation of GNP SAMs on fiber probes

Gold nanoparticles were bound to amine functionalized U-bent fiber probes as described below. A silanized U-bent sensor probe with bend radius of 0.75 mm was positioned between the source and detector with bend region of sensor probe in a custom-made L-shaped glass capillary of 2.5 mm diameter. The capillary tube was used to incubate the probe with GNP solution and also to subject the probes to solutions with different refractive indices at later stages of the experiments. The GNP solution was introduced into the capillary and absorbance spectrum was monitored in real-time. A linear increase in absorbance at 540 nm was observed as shown in Fig. 1 (inset). The peak absorbance of spectrum reached nearly three units within a time span of 30–60 min of incubation. Above an absorbance of about 2.5–3 units, the high absorption of light at the peak absorption wavelength of GNP led to a low SNR, which coupled to the spectral characteristics of the commercial LED used in these experiments, gave rise to a noisy signal. After one hour of incubation, fiber probes were washed with DI water. The absorbance spectrum recorded from the probe was as shown in Fig. 1.

The spectral characteristics of GNP coated fibers were slightly different from that of GNP in solution phase. A red shift in the peak wavelength and a broadening of spectrum was noticed in the spectrum. Further a plateau centered at 650 nm was observed in the spectrum. The red shift in the peak wavelength was observed from the beginning of the deposition of GNP onto the sensor probe. An average red shift of 13.4 ± 1.4 nm was observed. In similar study by Nath and Chilkoti (2004), no red shift has been reported. In fact, the occurrence of red shift is due to plasmon coupling between the chemisorbed GNP with the interparticle distance less than ~2.5 times the particle size (Jensen et al., 1999; Su et al., 2003). Hence, the cause for red shift in the spectrum is attributed to plasmon coupling between the nanoparticles resulting from high surface density. This argument is further supported by an increase in the red shift with the rise in the absorbance recorded from the fiber probe (Figure S-4). The plateau, observed at 650 nm in addition to the red shift, may have resulted from aggregation of GNP due to higher surface roughness of aminosilane layer on fiber and/or the size distribution of nanoparticles (Bar et al., 1996; Frederix et al., 2003; Grabar et al., 1995).

Our aim was to investigate the effectiveness of the GNP coated probes in detection of refractive index changes in the bulk as well microenvironment around the fiber probe by means of measurement of absorbance changes.

3.2. Absorbance sensitivity to refractive index changes

Subsequently, GNP coated probes were used for testing the bulk refractive index sensitivity. Since the spectral range of interest is around 540 nm, a light source restricted in the spectral range might be sufficient to achieve desired sensitivity in measuring refractive indices. In order to achieve higher SNR, a high intensity, commercially available green LED (peak: 525 nm; FWHM: 50 nm) was used as the light source. The integration time was also increased to aid in this effort. Sucrose solutions of different concentrations with refractive index between 1.33 and 1.40 were introduced and absorbance response was recorded. Fig. 2a shows the absorbance spectra obtained by subjecting the GNP coated sensor probe with consecutively higher % (w/w) sucrose solutions with RI varying from 1.33 to 1.35. A significant rise in absorbance was obtained for different RI solutions. However, no significant shift in peak wavelength was observed.

Bare U-bent probes are known to be sensitive to refractive index. In order to investigate the contribution of bending alone in the absorbance response, a bare bent probe of 0.5 mm radii and later the same probe coated with GNP were subjected to RI variation between 1.33 and 1.40 and absorbance response at 540 nm was monitored. The bare probe was found to induce a change in absorbance that is approximately one tenth of the absorbance obtained in presence of GNP monolayer. This trend was observed for entire range of refractive indices as shown in Fig. 2b. An important observation was the limitation of range of the RI detection between 1.33 and 1.38 RIU in aqueous phase. Effective light coupling between U-bent probe and GNP as well as significant absorption of light in presence of high RI solutions led to peak absorbance values of more than 2.5 units for RI of above 1.38. This resulted in poor signal to noise ratio in the output as < 0.001% of the light launched from an LED into the probe is transmitted to the detector end.

U-bent probes with radii 0.5 mm and 0.75 mm were coated with gold nanoparticles and tested with sucrose solutions to obtain information about sensitivity and resolution of probes for refractive index measurements. Sensitivity, defined as the ratio of the change in absorbance to the change in RI, was found to be linear between 1.33 and 1.35 RIU as shown in Fig. 2c. Sensitivity was found to be influenced by the bend radius of the probe with its value of 28.98 and 35.19 ΔA_{540nm}/RIU for 0.5 mm and 0.75 mm probes respectively.

3.3. Effect of bend radius on sensitivity

Results from the previous section and Fig. 2 indicate the dependence of sensitivity and resolution of U-bent probes on their bend radii. Previously, a variation in the sensor response of U-bent probes with respect to the bend diameter has been observed by Gupta and co-workers (Khijwania and Gupta, 2000). Thus, the sensitivity of the U-bent probes may be improved by exploring its optimum bend radius. Hence, U-bent probes with different radii were fabricated and their RI sensitivity was investigated. Results obtained in this study are shown in Fig. 3. An increase in the RI sensitivity was observed as the bend radius was reduced from 1.7 to 0.75 mm.

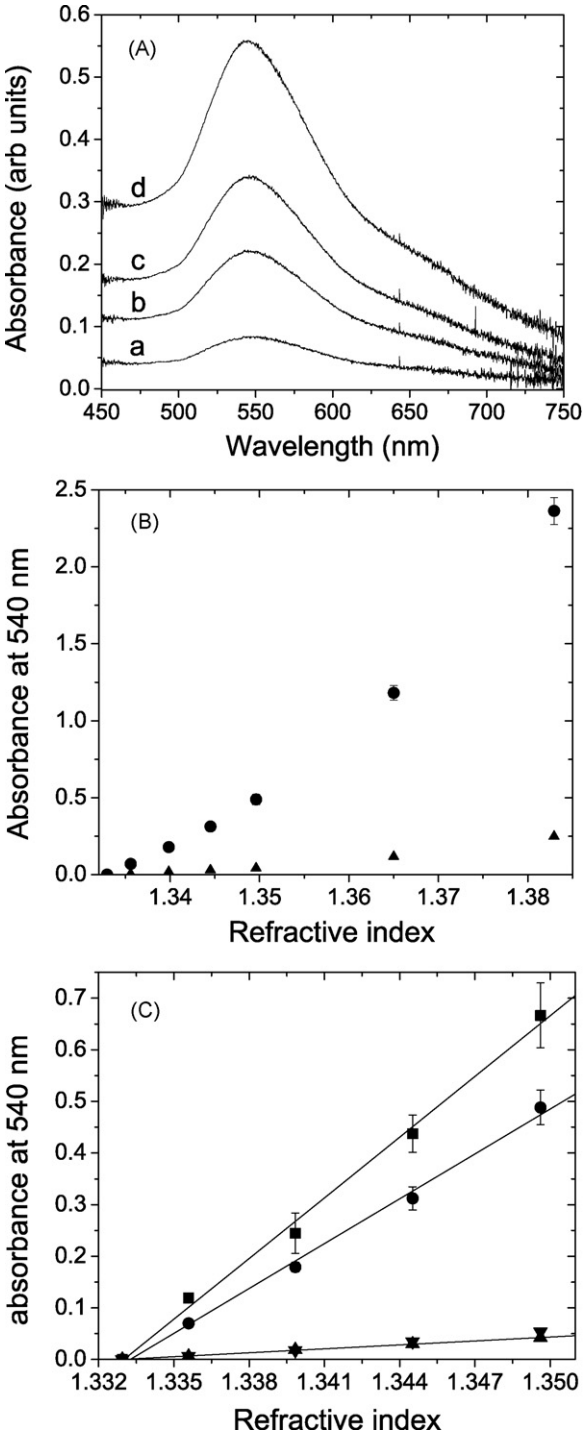

Fig. 2. (A) Absorbance spectra obtained for sucrose solutions with refractive index values (a) 1.3359, (b) 1.3403 (c) 1.3433 (d) 1.3494 (B) Absorbance response obtained from bare (▲) and GNP coated (●) U-bend probes of 0.5 mm radii in presence of media of different refractive indices ranging from 1.33 to 1.38 (C) Sensitivity of GNP bound U-bent probes of radii 0.5 mm (●) and 0.75 (■) mm and the corresponding bare probes 0.5 mm (▲) and 0.75 mm (▼) to RI changes at the probe surface between 1.33 and 1.35. A linear fit for the absorbance responses obtained for the two probes resulted in a slope or sensitivity 28.98 and 35.19 with R^2 = 0.9979 and 0.9976 respectively. A linear fit for bare probes gave a sensitivity of 2.55 with R^2 = 0.9986. (n = 3).

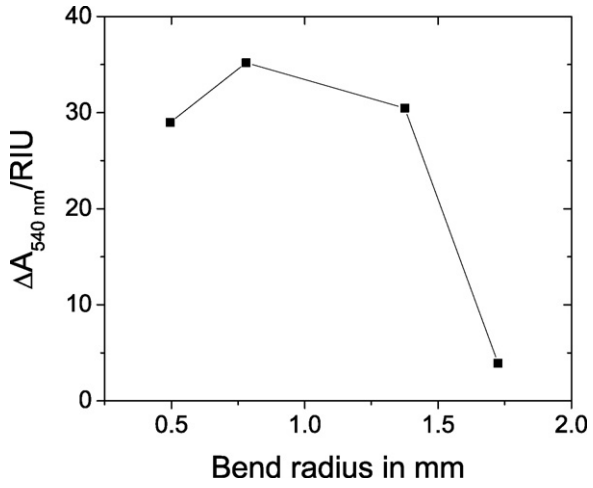

Fig. 3. Dependence of sensitivity (ΔA/RIU) of U-bent probes on bend diameter. Absorbance changes were measured from U-bent probes of different diameters by subjecting them to various % (w/w) sucrose solutions and slope of the linear fit was taken as the sensitivity of the probes.

This rise in sensitivity may be attributed to conversion of additional number of lower order modes to higher order modes with increasing bend radius. However, for the bend radius below 0.75 mm, sensitivity reduced due to higher losses at the bend region. The sensitivity of the probes of 1.7 mm radius was an order lower than that of 0.75 mm and similar to that of 2 cm long GNP coated straight probes (Figure S-6). Hence, we conclude that U-shaped bending of fiber probes may be effective for bend radii below 1.7 mm.

3.4. Biosensor applications

Immobilization of bioreceptors and immunocomplex formation during analyte binding on the surface of gold nanoparticles leads to increase in effective refractive index of the microenvironment. It results in increase in the optical absorbance of the gold nanoparticles. The ability of GNP coated U-bent probes in detecting these absorbance changes was tested by using IgG–anti IgG as bioreceptor–analyte pair. In order to minimize the probe-to-probe variation in the sensor response, U-bent probes of 0.5 mm bend radii were used in these studies due to their repeatability in the fabrication. U-bent fiber probes were silanized and incubated in gold nanoparticle solution and washed with DI water after 45 min. Gold nanoparticles were functionalized by incubating the probes in 5 mM cystamine prepared in absolute ethanol for 60 min, followed by 1% glutaraldehyde solution in water for 30 min. Human immunoglobulin G (HIgG) was immobilized on the functionalized probes by dipping in 0.1 mg/mL of HIgG in PBS for 4 h. HIgG Immobilized probes were treated with 2 mg/mL BSA to reduce non-specific binding followed by incubation with F_c specific goat anti-human IgG (GaHIgG). Interestingly, a downward shift in the peak absorbance was recorded during the incubation of probes in BSA solution. We attribute it to the difference in the refractive index values of PBS and BSA. PBS and 2 mg/mL BSA solution prepared PBS were experimentally found to have refractive index values of 1.3347 and 1.3331 respectively at 589.3 nm (measurements carried out with Pulfrich refractometer). Due to the sensitivity of GNP coated U-bent probe to bulk refractive index changes, we expect that the change in refractive index of the medium might have caused a shift in the absorbance value. The drop in the absorbance value was found to be in the order of the theoretical value obtained from multiplication of RI sensitivity of the probe and difference in the refractive index values of PBS and BSA. Absorbance change at 540 nm due to binding of HIgG and BSA was found to be 0.1 ± 0.006

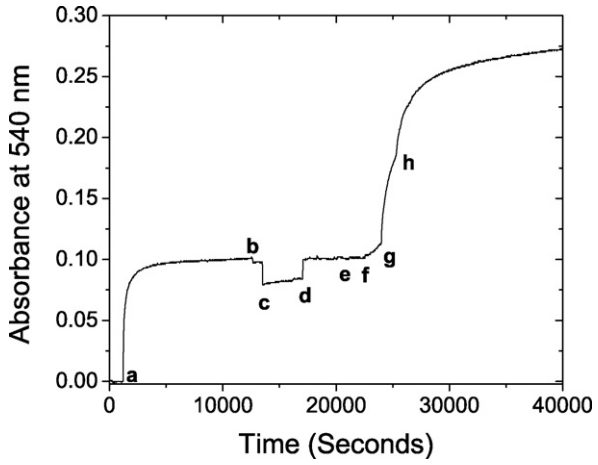

Fig. 4. Real time changes in absorbance recorded from a GNP coated U-bent fiber probe of 0.5 mm bend radius during binding of IgG–anti IgG. (a) Aldehyde functionalized GNP coated probe was incubated with 0.1 mg/mL of Human IgG (HIgG); (b) washed with PBS; (c) incubated with 2 mg/mL BSA in PBS and (d) finally washed with PBS. HIgG immobilized probes were subjected to (e) 0.06 μg/mL; (f) 0.6 μg/mL; (g) 6 μg/mL for 20 min followed by (h) 30 μg/mL until saturation is obtained.

and 0.005 ± 0.001 respectively (Fig. 4). The saturated absorbance response due to binding of GaHIgG to immobilized HIgG was 0.15 ± 0.02.

HIgG immobilized probes were tested with different concentrations of GaHIgG ranging between 0.1 and 15 μg/mL. The absorbance response was observed for 3 h to test the ability of the probes for real-time continuous monitoring. The real time absorbance changes at 540 nm from different probes were as shown in Fig. 5. It is important to note that saturated or steady state response was not obtained before of 3 h of incubation. In another study, a similar steady rise in the absorbance for lower analyte concentrations has been observed throughout the detection span (Nath and Chilkoti, 2004). Saturation or steady state response depends on the availability of free binding sites and/or analyte molecules to the probe. The response obtained in this study probably indicates that a larger number of binding sites are available on the probe surface compared to the analyte molecules available to bind to them. A slow rate of diffusion through a comparatively large analyte space may also contribute to the slow

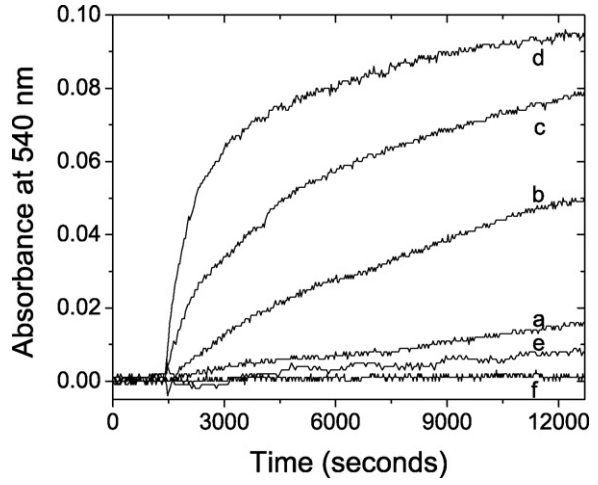

Fig. 5. Absorbance changes monitored at 540 nm caused by binding of anti-human IgG to human IgG immobilized GNP coated U-bent fiber probes of 0.5 mm bend radii for (a) 0.12 μg/mL, (b) 0.6 μg/mL, (c) 6 μg/mL and (d) 15 μg/mL of goat anti-human IgG. (e) Absorbance due to non-specific binding of anti human IgG to rabbit IgG immobilized probe. (f) Baseline response of HIgG immobilized probe observed for 3 h in presence of PBS.

increase after the initial rise. To test the non-specific binding, sensor probe was immobilized with rabbit IgG. Absorbance response was monitored in presence of 6 μg/mL of goat anti-human IgG. The rise in absorbance due to non-specific binding was found be less than half that of specific binding of 0.12 μg/mL of goat anti-human IgG. Hence, U-bent probes of 0.5 mm bent radius were capable of detecting a concentration of 0.12 μg/mL (0.8 nM) of the analyte.

4. Discussion

The sensitivity obtained using GNP coated U-bent probes was 30 times better than that of nanoSPR sensors consisting of GNP coated cover glass substrates (Nath and Chilkoti, 2004). The resolution of sensor probes were calculated as 3.8×10^{-5} RIU and 5.2×10^{-5} RIU for 0.75 mm and 0.5 mm probes respectively (assuming an ability to detect 0.0015 abs units). The improved resolution using the bent probes was 15 times that of LSPR based 400 μm diameter, 5 cm long straight fiber optic biochemical probes and similar that of distal end sensor configuration with 50 μm core fiber (Chau et al., 2006; Mitsui et al., 2004). Although a superior sensitivity and resolution has been reported by using long range SPR and LSPR coupled with interferometry (Slavík and Homola, 2007; Kim et al., 2007), there is a wide scope for improvement in the performance of the U-bent probes by optimizing different sensor parameters as described below.

The knowledge of different parameters that influence the performance of evanescent wave absorbance based sensor can be obtained by the following equation. Evanescent absorbance, A, in case of a fiber optic sensor is given by (Ruddy et al., 1990),

$$A = k \cdot \frac{\sqrt{2} \cdot 4\lambda}{3 \cdot 2\pi \cdot r \cdot \mathrm{NA}} \cdot \varepsilon_{\mathrm{ex}} CL \quad (1)$$

where, r is the radius of the optical fiber into which light is coupled, NA is the numerical aperture at the sensing region of the fiber, λ is the wavelength of light, $\varepsilon_{\mathrm{ex}}$ is the extinction coefficient of absorbing medium (GNP), and C is the concentration of absorbent molecules bound per unit circumferential surface area of the fiber. We have introduced k as a correction factor in order to take into account the possible saturation in the absorbance response due to the limitations of confined influence of evanescent field on the limited surface density of chromophores i.e. a monolayer of GNP around the fiber core.

From Eq. (1) and reported literature, it is understood that sensitivity of GNP coated U-bent probes can be improved by optimization of influential parameters, such as the size and surface coverage of gold nanoparticles and probe geometry including fiber diameter, probe length and bend radius (Khijwania and Gupta, 2000). Nath and Chilkoti (2004) have experimentally verified the dependence of RI sensitivity on surface particle density. A highest RI sensitivity has been obtained with GNP of 39 nm. In our experiments, a surface coverage of GNP (~40 nm size) on sensor probe was restricted to a peak absorbance of 3 units due to limitation of poor signal-to-noise ratio in the absorbance measurements beyond that value. Hence, it is unlikely for GNP coated U-bent probes to achieve any further improvement in sensor performance by varying the size and surface coverage of GNP. However, sensor response may be enhanced by modifying the geometry of U-bent probes. The optimum bent radius for 200 μm core diameter was investigated in this study. In case of GNP coated straight fiber probes, a length of 5 cm was found to give rise to linear response to refractive index changes (Chau et al., 2006). The overall and effective probe lengths in this study were 2 and 1 cm respectively. Hence, we expect two- or three-fold improvement in resolution of refractive index by optimizing the probe length. It may be foreseen that the sensitivity will increase and probably double if optical fiber probes with 100 μm diameter are used. Thus, it may be possible to obtain a resolution of better

than 10^{-5} RIU. However, the complexities involved in the use of longer probe lengths and reduced fiber diameter, such as necessity of higher sample volume and difficulty in handling of the probes, should be taken into account.

Apart from gold nanoparticles, a high RI sensitivity may be obtained by incorporating gold colloids with higher extinction coefficient such as nanostars, nanorice and nanorods on U-bent probes (Nehl et al., 2006; Wang et al., 2006; Muskens et al., 2008). Similar to nanospheres, absorption/scattering spectrum of the other gold colloids can be fine-tuned by varying the aspect ratio (Muskens et al., 2008). In addition, the extinction properties of these gold colloids in near infrared (NIR) region also may aid in enhancement in the sensor response due to the dependence of evanescent wave absorbance on the wavelength of operation (Eq. (1)).

5. Conclusion

We have demonstrated use of novel U-bent fiber optic probes for absorbance based LSPR sensor applications. They are capable of detecting bulk refractive index changes with a sensitivity and resolution of 35.19 A_{540nm}/RIU and 3.8×10^{-5} RIU respectively. The results obtained in case of biosensor applications were promising with minimum detection limit of 0.8 nM of anti-IgG. Compared to conventional SPR sensors, the preparation of these sensor probes is far simpler, easily executable in ordinary laboratory conditions and less expensive. Further studies are in progress to realize a complete, portable and field suitable biosensing system with a better sensitivity using a green/white LED, a photodetector and supporting electronics with few additional optical components.

Acknowledgements

This research was supported by grants from NMRL, India and DIT, Govt. of India. We thank Sophisticated Analytical Instrument Facility (SAIF), IIT Bombay for TEM images acquired in support of this study. VVR Sai thanks Deepu A., Kamini Thakare and Arvind Dhanwangale for their help.

Appendix A. Supplementary data

Supplementary data associated with this article can be found, in the online version, at doi:10.1016/j.bios.2009.02.007.

References

Bar, G., Rubin, S., Cutts, R.W., Taylor, T.N., Zawodzinski, T.A., 1996. Langmuir 12, 1172–1179.
Chau, L.-K., Lin, Y.-F., Cheng, S.-F., Lin, T.-J., 2006. Sensors and Actuators B 113, 100–105.
Cooper, M.A., 2006. Drug Discovery Today 11, 1061–1067.
Endo, T., Kerman, K., Nagatani, N., Takamura, Y., Tamiya, E., 2005. Analytical Chemistry 77 (21), 6976–6984.
Englebienne, P., 1998. Analyst 123, 1599–1603.
Frederix, F., Friedt, J.-M., Choi, K.-H., Laureyn, W., Campitelli, A., Mondelaers, D., Maes, G., Borghs, G., 2003. Analytical Chemistry 75, 6894–6900.
Grabar, K.C., Freeman, R.G., Hommer, M.B., Natan, M.J., 1995. Analytical Chemistry 67, 735–743.
Gupta, B.D., Dodeja, H., Tomar, A.K., 1996. Optical and Quantum Electronics 28, 1629–1639.
Homola, J., 2006. Surface Plasmon Resonance based Sensors: Springer Series on Chemical Sensors and Biosensors. Springer-Verlag, Heidelberg.
Homola, J., 2008. Chemical Reviews 108 (2), 462–493.
Jain, P.K., Huang, X., El-Sayed, I.H., El-Sayed, M.A., 2007. Plasmonics 2 (3), 107–118.
Jensen, T., Kelly, L., Lazarides, A., Schatz, G.C., 1999. Journal of Cluster Science 10, 295–317.
Tang, J.-L., Cheng, S.-F., Hsu, W.-T., Chiang, T.-Y., Chau, L.-K., 2006. Sensors and Actuators B: Chemical 119 (1), 105–109.
Khijwania, S.K., Gupta, B.D., 1998. Optics Communications 152, 259–262.
Khijwania, S.K., Gupta, B.D., 2000. Optical Communications 175, 135–137.
Kim, D.-K., Kerman, K., Saito, M., Sathuluri, R.R., Endo, T., Yamamura, S., Kwon, Y.-S., Tamiya, E., 2007. Analytical Chemistry 79 (5), 1855–1864.
Leung, A., Shankar, P.M., Mutharasan, R., 2007. Sensors and Actuators B: Chemical 125, 688–703.
Lin, H.-Y., Chen, C.-T., Chen, Y.-C., 2006. Analytical Chemistry 78, 6873–6878.
Littlejohn, D., Lucas, D., Han, L., 1999. Applied Spectroscopy 53 (7), 845–849.
Mitsui, K., Handa, Y., Kajikawa, K., 2004. Applied Physics Letters 85 (18), 4231–4233.
Muskens, O.L., Bachelier, G., Fatti, N.D., Valleĭe, F., Brioude, A., Jiang, X., Pileni, M.-P., 2008. Journal of Physical Chemistry C 112 (24), 8917–8921.
Nath, N., Chilkoti, A., 2002. Analytical Chemistry 74, 504–509.
Nath, N., Chilkoti, A., 2004. Analytical Chemistry 76, 5370–5378.
Nehl, C.L., Liao, H.W., Hafner, J.H., 2006. Nano Letters 6, 683–688.
Okamoto, T., Yamaguchi, I., Kobayashi, T., 2000. Optics Letters 25, 372–374.
Prasad, B., 1999. Capacitive immunosensors for fibronectin. Ph.D. Thesis. IIT Bombay, chapter 3.
Ruddy, V., MacCraith, B.D., Murphy, J.A., 1990. Journal of Applied Physics 67 (10), 6070–6074.
Slavík, R., Homola, J., 2007. Sensors and Actuators B: Chemical 123, 10–12.
Su, K.H., Wei, Q.H., Zhang, X., Mock, J.J., Smith, D.R., Schultz, S., 2003. Nano Letters 3, 1087–1090. <http://pubs.acs.org/cgi-bin/citation?nalefd/3/i08/html/nl034197f.html>.
Turkevich, J., Stevenson, P.C., Hiller, J., 1951. Discussions of Faraday Society 11, 55–75.
Wang, H., Brandl, D.W., Le, F., Nordlander, P., Halas, N.J., 2006. Nano Letters 6, 827–832.
Wei, P.K., Chang, Y.J., Lee, C.W., 2006. Progress in Biomedical Optics and Imaging—Proceedings of SPIE 6099.